

Journal of Materials Chemistry A

Accepted Manuscript



This is an *Accepted Manuscript*, which has been through the Royal Society of Chemistry peer review process and has been accepted for publication.

Accepted Manuscripts are published online shortly after acceptance, before technical editing, formatting and proof reading. Using this free service, authors can make their results available to the community, in citable form, before we publish the edited article. We will replace this *Accepted Manuscript* with the edited and formatted *Advance Article* as soon as it is available.

You can find more information about *Accepted Manuscripts* in the [Information for Authors](#).

Please note that technical editing may introduce minor changes to the text and/or graphics, which may alter content. The journal's standard [Terms & Conditions](#) and the [Ethical guidelines](#) still apply. In no event shall the Royal Society of Chemistry be held responsible for any errors or omissions in this *Accepted Manuscript* or any consequences arising from the use of any information it contains.

ARTICLE

Limiting factors for photochemical charge separation in BiVO₄/Co₃O₄, a highly active photocatalyst for water oxidation in sunlight

Cite this: DOI: 10.1039/x0xx00000x

Received 00th January 2014,

Accepted 00th January 2014

DOI: 10.1039/x0xx00000x

www.rsc.org/

Jiarui Wang^a and Frank E. Osterloh^a

Chemical modification of BiVO₄ nanoparticles (Scheelite, E_G=2.62 eV) with chemically deposited Co₃O₄ nanoparticles improves the photocatalytic water oxidation activity by a factor of 17 to 11 mmol g⁻¹h⁻¹ under visible light (AQE 10% at 435 nm) and to 1.24 mmol g⁻¹h⁻¹ under sunlight from aqueous 0.02 M NaIO₄. This activity ranks among the highest among known visible light driven water oxidation photocatalysts. Based on systematic electrochemical, photoelectrochemical, and surface photovoltage measurements, the high photocatalytic activity can be attributed to the electrocatalytic properties of the Co₃O₄ cocatalyst and to the formation of heterojunction at the BiVO₄-Co₃O₄ interface.

Introduction

The photocatalytic water splitting reaction is a carbon-free pathway to generate hydrogen fuel from abundant sunlight and water. Potentially, powdered catalysts¹⁻³ are the most economical way to drive this process.⁴ Due to its chemical stability, 2.4 eV band gap, and n-type character, bismuth vanadate is a promising photoanode material for water oxidation - one half reaction in water photoelectrolysis.⁵ Since its first report in 1998 by Kudo et al.,⁶ several structure types and morphologies of BiVO₄ have been reported for water oxidation.⁷⁻¹¹ It also has been established that the efficiency of unmodified BiVO₄ is limited by electron-hole recombination, slow carrier transport, and slow water oxidation kinetics.^{12, 13} Doping with molybdenum^{14, 15} or tungsten,¹⁶ addition of cocatalysts (Co-Pi^{15, 17, 18}, FeOOH¹⁹, nanostructuring^{19, 20} and junction formation⁵ have been explored to address these problems. In 2006, Long et al. reported that the addition of Co₃O₄ to BiVO₄ increased the activity for *phenol oxidation*.^{10, 21} As we show here, the addition of Co₃O₄ also leads to 17 times improved photocatalytic *water oxidation* with BiVO₄. After optimization of the Co₃O₄ content, suspended BiVO₄-Co₃O₄ (1%) composite particles catalyze water oxidation with under visible light (380 mW cm⁻², 11 mmol g⁻¹h⁻¹) and direct sunlight (1.24 mmol g⁻¹h⁻¹). The quantum efficiency is 10% at 435 nm. Surface photovoltage spectra and electrochemical and photoelectrochemical data show that the improved performance can be attributed to the reduction of the water oxidation potential by Co₃O₄^{10, 22} and to the formation of BiVO₄-Co₃O₄ junction that aids electron-hole separation, and that creates a photovoltage of about 12 mV. This work sheds light on the

importance of the light absorber – cocatalyst interfaces for achieving optimal charge separation in suspended water oxidation photocatalysts.

Results and discussion

Electron micrographs of BiVO₄ particles (Details in Supporting Information), made by solid-solution reaction and after calcination at 673 K²³ are shown in Figure 1A. The particles have round features and sizes of 73 ± 35 nm and that are clustered into agglomerates. X-ray diffraction suggests the presence of the monoclinic Scheelite phase (Figure S1). Optical measurements (Figure 2) reveal an indirect and direct band gap of 2.45 eV and 2.62 eV, respectively, slightly higher than reported earlier (2.28 eV).²¹

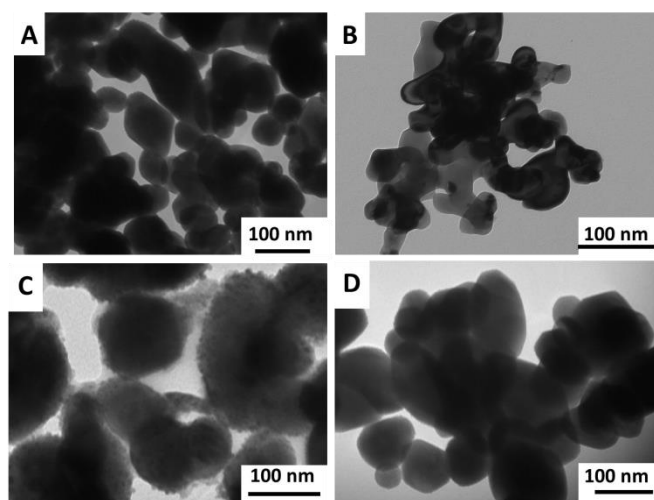


Figure 1. TEM images of (A) BiVO_4 , (B) commercial Co_3O_4 particles (C) Chem- Co_3O_4 - BiVO_4 and (D) Phys- Co_3O_4 - BiVO_4

The optical properties of BiVO_4 and the composites are summarized in Figure 2. The indirect and direct band gap of BiVO_4 was found as 2.45 eV and 2.62 eV by Tauc plot. This value is slightly higher than reported earlier (2.28 eV).²¹ The introduction of the Co_3O_4 phase leads to a grey-yellow appearance of Chem- Co_3O_4 - BiVO_4 , which is due to a broad absorption at 500 - 900 nm (Figure 2A) characteristic of the Co_3O_4 phase.¹⁸ For Phys- Co_3O_4 - BiVO_4 , this absorption is obscured by scattering.

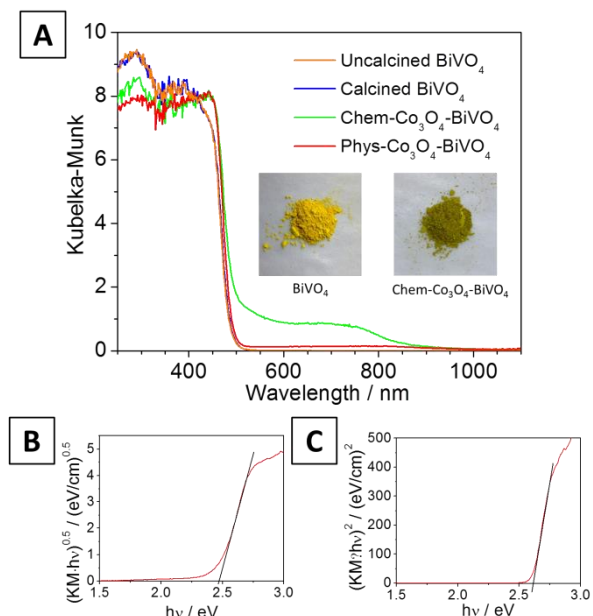


Figure 2. UV-Vis spectra and photos of BiVO_4 with cocatalysts (A) and Tauc plots for allowed indirect transitions (B) and direct transitions (C) of calcined BiVO_4 .

As will be shown in the following, BiVO_4 - Co_3O_4 is an active photocatalyst for water oxidation in the presence of a chemical or electrochemical bias. In order to find the optimum Co_3O_4 content, a series of Co_3O_4 - BiVO_4 samples were synthesized via an electrochemical route. Here, BiVO_4 electrodes were first prepared by drop-coating of the BiVO_4 powder on FTO coated glass substrates, and variable amounts (0.5, 1, 2 and 4 wt%) of cobalt metal were electrochemically deposited on to from 0.01 M $\text{Co}(\text{NO}_3)_2$ solution at a fixed current density of 0.2 mA/cm^2 . The electrodes were then rinsed with water, dried in air and calcined at 673 K for 5 hours to oxidize the cobalt to Co_3O_4 , and to produce thin films of composites, labeled as Echem- Co_3O_4 - BiVO_4 in the following. Electrochemical scans of the Echem- Co_3O_4 - BiVO_4 samples are shown in Figure 3A. All materials have much lower water oxidation potentials at 1 mA/cm^2 (1.35V to 1.6V vs NHE) than unmodified BiVO_4 (2.38 V vs NHE). This clearly showed that the added Co_3O_4 is an effective cocatalyst for water oxidation. The effect was most pronounced for the 4% Co_3O_4 containing sample, but even at 0.5 % Co_3O_4 a significant 0.9 V decrease of the water oxidation overpotential was observed.

To evaluate the effect of the Co_3O_4 cocatalyst on photoelectrochemical water oxidation, the photocurrent response of the Echem- Co_3O_4 - BiVO_4 films was observed in 0.1 M K_2SO_4 aqueous solution (Figure 3B) under illumination from 435 nm LED (7.4 mW/cm^2). All samples produce anodic photocurrents at applied potentials above +0.5 V (NHE). The addition of Co_3O_4 first decreases the photocurrent (at 0.5 % loading), then increases it at intermediate loading (1%), and then decreases it again at large loadings (2, 4%). Also, there are strong capacitive currents in the Co_3O_4 rich samples, as evident from the saw-tooth shape of the photocurrent response after switching the light. A magnified view of this current is shown in Figure 3C in the time domain. All of these findings can be explained with the model shown in the insert of Figure 3C. The capacitive charge Q is due to the trapping and detrapping of photogenerated charge carriers in the asymmetric Co_3O_4 - BiVO_4 -FTO configuration. The charging is driven by the photopotential U that develops across the illuminated film. Only some of the photoholes are able to generate a faradic current due to water oxidation, while the remainder flows back into the BiVO_4 film when the light is turned off. The reduced faradaic photocurrents for the films with the highest Co_3O_4 loading can simply be explained from the shading effect of the Co_3O_4 layer.

In contrast, Chem/Phys- Co_3O_4 - BiVO_4 catalyst samples prepared by chemical or physical deposition of Co_3O_4 showed much cleaner photochemistry (Figure 3D). In both figures, the positive effect of the added Co_3O_4 can be observed clearly. The Co_3O_4 cocatalyst works as the hole collector and provides a fast path for the charge transfer between the BiVO_4 light absorber and the solution. No capacitive currents are observed due to homogeneous mixing of the Co_3O_4 phase with the BiVO_4 film.

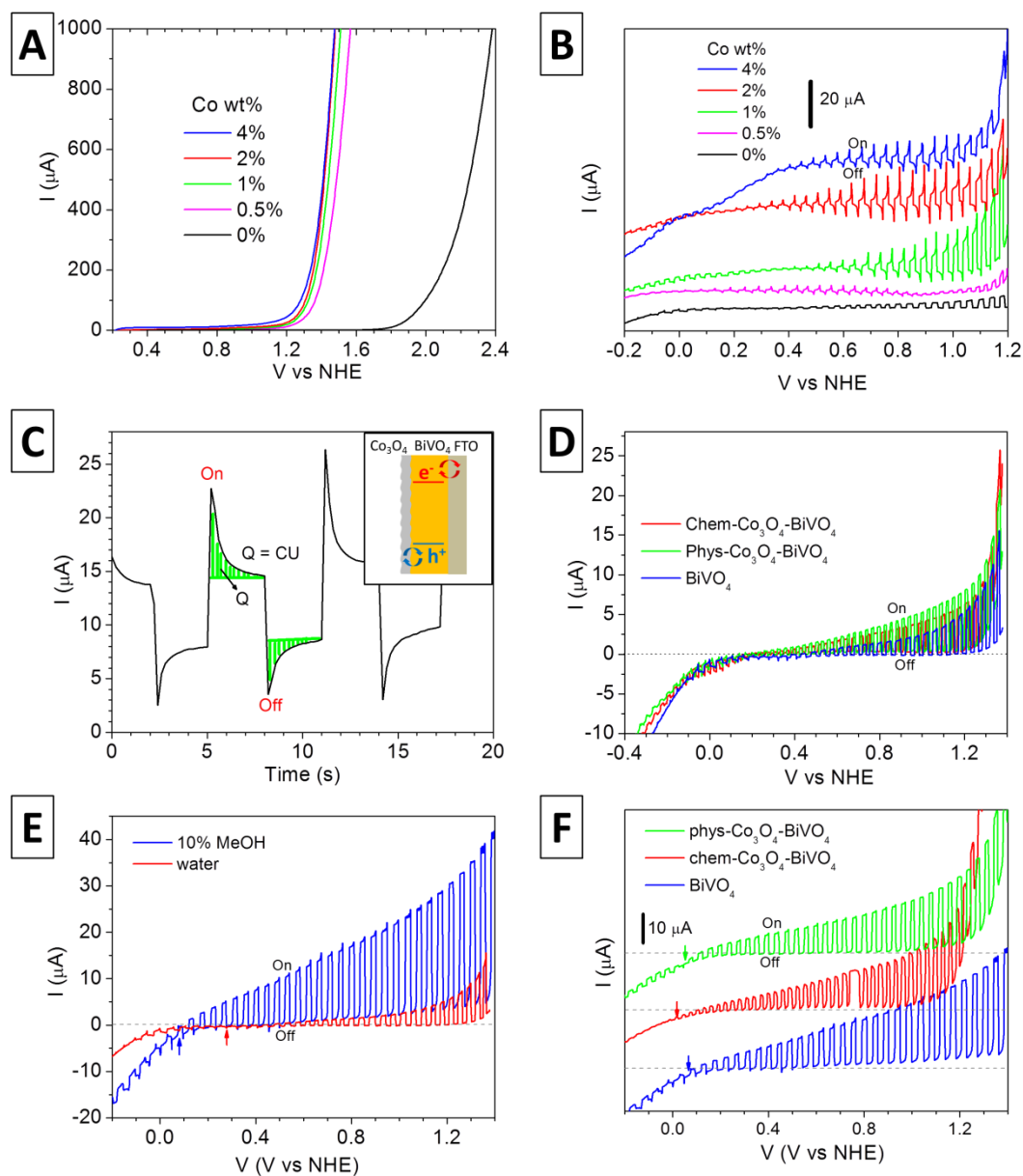


Figure 3. (A) Dependence of overvoltage on Co_3O_4 content in dark, (B) Photoelectrochemical scans of Echem- Co_3O_4 - BiVO_4 with different amount of Co_3O_4 , (C) Capacitive current of 2 wt% Co Echem- Co_3O_4 - BiVO_4 (0.9 V to 0.7 V, 10 mV/s), (D) Photoelectrochemical scans of Phys-/Chem- Co_3O_4 - BiVO_4 and BiVO_4 , (A to D were measured in 0.1 M K_2SO_4 aqueous solution) (E) Comparison of photoelectrochemical scans of BiVO_4 in 0.1 M K_2SO_4 10 vol% methanol aqueous solution and water solution, (F) Photoelectrochemical scans (0.1 M K_2SO_4 10 vol% methanol aqueous solution) of modified BiVO_4 . (All electrodes are prepared with 0.5 mg catalyst on 1 cm^2 FTO substrate)

Based on the photoelectrochemical data, suspensions of Co_3O_4 - BiVO_4 should catalyze water oxidation when illuminated in the presence of a chemical bias. Accordingly, 50 mg of each catalyst were suspended in 50 mL of aqueous 0.05 M AgNO_3 ($E^0=0.80 \text{ V NHE}$)²⁴ or 0.02 M NaIO_4 ($E^0=1.60 \text{ V NHE}$),²⁵ and irradiated with visible light (Xe lamp, 380 mW cm^{-2} , $>400 \text{ nm}$). Both reagents promote light-induced oxygen formation (Figure

4A) at comparable rates, but in the presence of AgNO_3 the activity quickly falls off to zero. This is due to chemical deposition of silver metal, which also produces a dark grey coloration and aggregation of the sample. On the other hand, the rate of NaIO_4 sample stays constant during the eight-hour experiment and reaches $620 \mu\text{mol} \cdot \text{g}^{-1} \cdot \text{h}^{-1}$. No O_2 was evolved in dark or when NaIO_4 was illuminated with Co_3O_4 only.

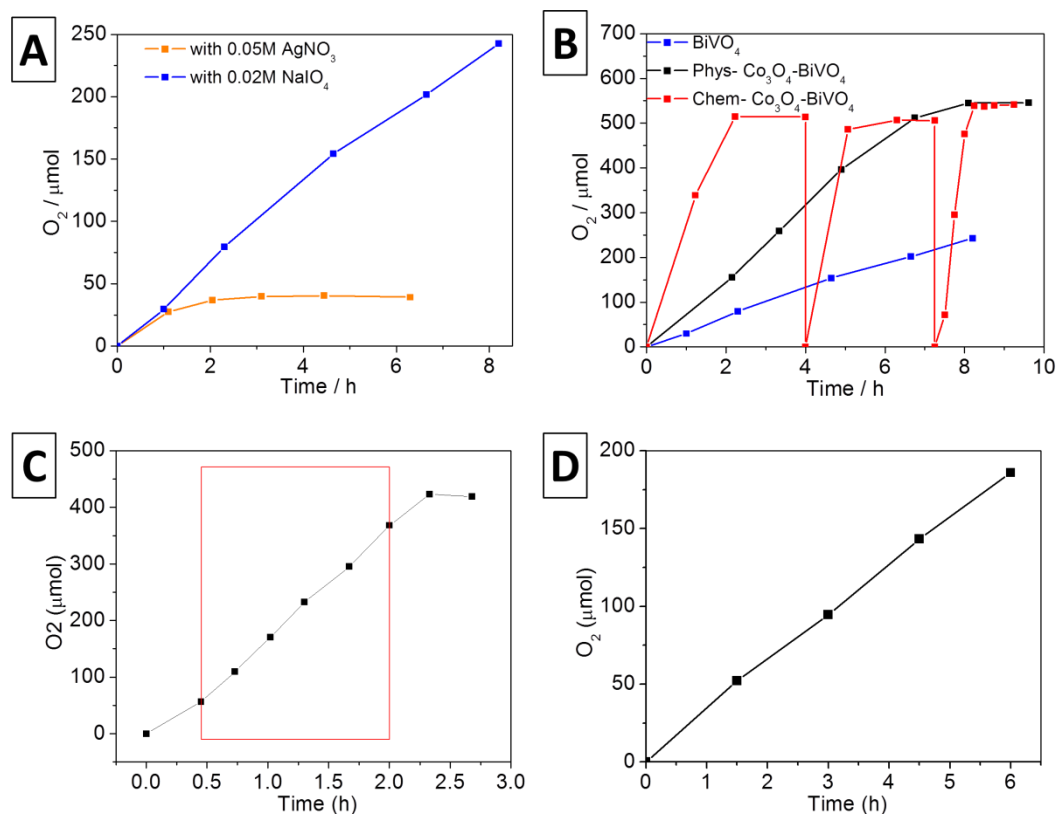


Figure 4. Oxygen evolution from (A) BiVO₄ in 0.05 M aqueous AgNO₃ and 0.02 M NaIO₄ and (B) from BiVO₄-Co₃O₄ in 0.02 M aqueous NaIO₄ (50 mg catalyst in 50 mL solution under light from Xe lamp at 380 mW cm⁻² and with 400 nm long pass filter). (C) For the AQE measurement a 435 nm LED, 249 mW/cm² by 2.54 cm² was used. (D) O₂ evolution from 15 mg BiVO₄/Co₃O₄ in 50 mL of 0.02 M aqueous NaIO₄ under sunlight.

Figure 4B shows a comparison of O₂ evolution from Co₃O₄-BiVO₄ with chemically (CD) or physically deposited (PD) Co₃O₄. The reactivity increases in the order BiVO₄ (blue) < Phys-Co₃O₄-BiVO₄ (black) < Chem- Co₃O₄-BiVO₄ (blue). Within 2 hours, the NaIO₄ is used up, and replaced with fresh reagent to fully re-establish O₂ production, without any decrease in activity. For the third run, the rate was calculated to be 11 mmol g⁻¹h⁻¹, which is 17 times greater than for unmodified BiVO₄. This activity ranks among the highest among known visible light driven water oxidation photocatalysts (Table S1). The turnover number was 189 (based on BiVO₄) for the three tests, and the apparent quantum efficiency (AQE) is 10 % at 435 nm (Figure 4C) based on the data from 0.45 h in the 0.5-2.0 h interval (red box). The Co₃O₄-BiVO₄ catalyst was also tested under sunlight in Davis, CA to yield O₂ at an average rate of 1.24 mmol g⁻¹h⁻¹. The lower rate is a result of the lower illumination power (76 mW/cm², calculation in Supporting information) under the conditions employed.

In order to further investigate charge transfer in the Co₃O₄-BiVO₄ composites, surface photovoltage spectroscopy (SPS) was employed.^{26,27} Here, a contact-less Kelvin probe is used to record the light-induced changes in the contact potential as a function of the excitation energy (Figure 5A). This can provide insight into photochemical charge transfer in solids,²⁸ at solid-

solid²⁹ and solid-gas³⁰ interfaces, involving inorganic, molecular³¹ and organic polymeric materials.³² Because of its high sensitivity³⁰ it is possible to observe states with low optical cross sections, including trap sites in nanoparticles,³³ interfacial³², and defect states.³⁴ That makes the technique particularly useful for the study of nanoparticles.^{30,35,36}

Spectra for nanoparticle films of Co₃O₄, BiVO₄, and Co₃O₄-BiVO₄ are shown in Figure 5B. Under illumination BiVO₄ alone (blue) produces a negative signal with an onset at 2.45 eV and a maximum photovoltage of ΔCPD = -0.014 V near 3.0 eV. This negative voltage indicates that electrons are moving towards the substrate and away from the Kelvin probe. The photoonset agrees with the optical band gap of the material, confirming that charge carriers are formed by band gap excitation. The spectrum for Chem-Co₃O₄-BiVO₄ (black) is similar, except that the curve has a larger steeper downward slope and the photovoltage is increased to -0.023 V at 3.0 eV. This indicates that the Co₃O₄ cocatalyst promotes hole accumulation in the film, likely through trapping on Co²⁺ sites. As a result, charge separation in the Co₃O₄-BiVO₄ system is improved. Under similar conditions the photovoltage of Phys-Co₃O₄-BiVO₄ (red) is reduced compared to that for BiVO₄. This indicates that hole-trapping is less effective in this material. The material also produces a positive CPD signal with a photoonset of 1.6 eV. This positive photovoltage signal below the BiVO₄ bandgap can be attributed to direct excitation of

Co_3O_4 . The spectrum for a pure Co_3O_4 film is shown in green. The 1.6 eV photoonset coincides with the onset of optical absorption of Co_3O_4 as seen at 800 nm (1.55 eV) in the optical spectrum in Figure 2A. The positive sign indicates hole transport towards the substrate,²⁹ which agrees well with the p-type character of Co_3O_4 .³⁷ The variable SPS behavior of Phys- and Chem- Co_3O_4 - BiVO_4 shows that the electronic interactions between the Co_3O_4 and BiVO_4 components in both materials are different. While the physically mixed sample contains electronically isolated components, the chemically deposited sample supports selective hole injection from BiVO_4 into Co_3O_4 . This suggests the formation of a p-n-heterojunction at the Chem- Co_3O_4 - BiVO_4 interface. The photopotential of this junction can be estimated as the difference between the contact potential of the Chem- Co_3O_4 - BiVO_4 sample and of the pure BiVO_4 and chem- Co_3O_4 components. At 3.0 eV, this value is $(-23 \text{ mV}) - (-14 \text{ mV}) - 3 \text{ mV} = -12 \text{ mV}$. This voltage promotes water oxidation under illumination of Chem- Co_3O_4 - BiVO_4 . It is the reason for the higher photocatalytic activity of Chem- Co_3O_4 - BiVO_4 compared to Phys- Co_3O_4 - BiVO_4 .

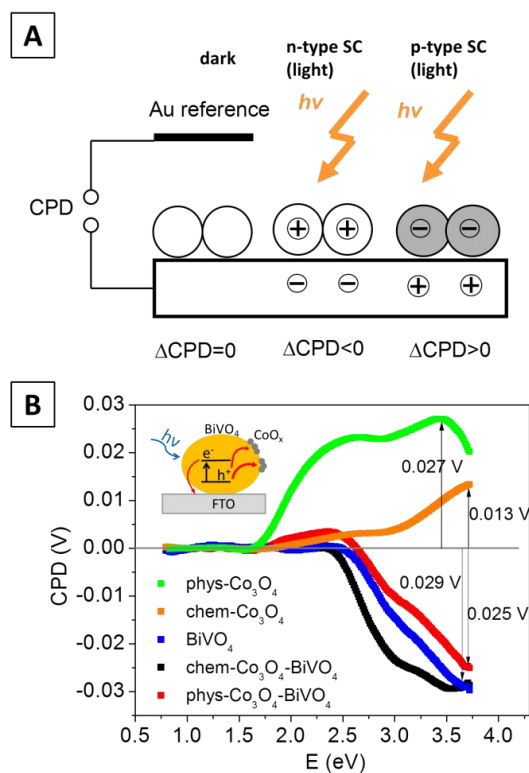


Figure 5. (A) Surface photovoltage geometry, (B) Surface photovoltage spectra of Phys- Co_3O_4 , Chem- Co_3O_4 , BiVO_4 , and Chem/Phys- Co_3O_4 - BiVO_4 (0.5 mg/cm^2) on FTO substrate in vacuum atmosphere (10^{-4} mbar), 175 W Xe lamp, 0.1 to 0.3 mW/cm^2

Lastly, the energetics of the Co_3O_4 - BiVO_4 composites was analyzed to help understand the driving force for photocatalysis. To obtain quasi-Fermi levels of the materials, photoelectrochemical scans for BiVO_4 and Co_3O_4 - BiVO_4 were

recorded with methanol as fast hole acceptor (Figure 3E and 3F). Under conditions of fast charge transfer at the solid-liquid interface, the photoonset potential is a good approximation of the quasi-Fermi level (electrochemical electron potential) of a semiconductor.³⁸ As can be seen from Figure 3E, the addition of 10 % methanol to the aqueous 0.1 M K_2SO_4 electrolyte increases the anodic photocurrent of the pure BiVO_4 film by a factor of 5, compared to the non-methanol case, and moves the onset potential 0.2 V into negative direction, to 0.1 V (NHE). In contrast, the photocurrents from chem/Phys- Co_3O_4 - BiVO_4 are slightly enhanced by the methanol (Figure 3F), and the negative shift of the onset potential is less than 0.1 V. This demonstrates that the performance of the composites is not limited by the water oxidation kinetics, but by other effects, including shading from Co_3O_4 , and probably increased electron hole recombination from Co_3O_4 - BiVO_4 interfacial states.

An energy scheme for the BiVO_4 / Co_3O_4 photocatalytic system is shown in Figure 6. The conduction band edge for BiVO_4 was calculated at 0.14 V vs NHE by the method of Butler and Ginley³⁹ using the optical band gap from the Kubelka-Munk spectra and after correcting for the deviation from the point of zero charge to pH 7 (Details in Supporting Information). The valence band for this compound lies at 2.83 V vs NHE. Similarly, with the 2.07 eV band gap of Co_3O_4 ,⁴⁰ conduction band edge and valence band edge of Co_3O_4 were calculated as 0.41 V and 2.48 V vs NHE. From the anodic photocurrent onset of BiVO_4 (Figure 4E and F) the quasi Fermi level of electrons, E_{Fn} is estimated around 0.1 V vs NHE (from 10% MeOH it is 0.1 V and without methanol it is 0.3 V). This value is close to the conduction band, which agrees with the n-type character of BiVO_4 .

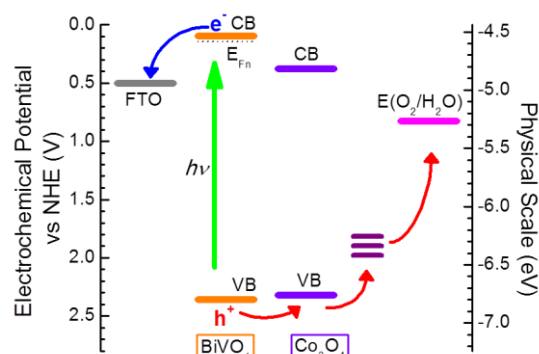


Figure 6. Energy scheme of BiVO_4 / Co_3O_4 photocatalytic system on electrochemical and vacuum scale at pH 7. Potential of $\text{Co}^{3+/2+}$ interfacial states estimated from $E^0(\text{Co}^{3+/2+}) = 1.92 \text{ V}$.²⁴

Based on the energy scheme in Figure 6, the migration of light-induced electrons to the FTO support is possible, which is coherent with the SPV spectra. Addition of the Co_3O_4 phase allows photoholes to leave BiVO_4 , causing the observed 12 mV increase in the photovoltage. Likely, the actual water oxidation reaction does not involve O states in the Co_3O_4 valence band,

but intermediate $\text{Co}^{3+/2+}$ species at the Co_3O_4 surface. These states lower the water oxidation overpotential, but at the same time they act as recombination sites for electron hole pairs at the Co_3O_4 - BiVO_4 interface. This is the reason for the low efficiency of the Co_3O_4 - BiVO_4 junction and the small photopotential resulting from it. Similar junctions are likely present in single-crystal BiVO_4 composites reported recently by Li et al.⁴¹

Conclusions

In conclusion we have shown that the addition of cobalt oxide to powdered BiVO_4 improves the photocatalytic water oxidation ability of this system to $11 \text{ mmol g}^{-1}\text{h}^{-1} \text{ O}_2$ from aqueous NaIO_4 solution under artificial visible light illumination ($1240 \mu\text{mol g}^{-1}\text{h}^{-1}$ under sunlight) and an apparent quantum yield of 10% (at 435 nm). This activity ranks among the highest among known visible light driven water oxidation photocatalysts. Electrochemical measurements confirm that Co_3O_4 improves the water oxidation kinetics and lowers the overpotential. SPS confirms p-type character for the Co_3O_4 particles and a junction at the Co_3O_4 - BiVO_4 interface. This junction improves electron-hole separation due to hole injection into Co_3O_4 and supports a photovoltage of $\sim 12 \text{ mV}$ at 3.0 eV . An analysis of the system energetics suggests that the activity of the catalyst can be improved further by eliminating mid gap states at the Co_3O_4 - BiVO_4 interface that are responsible for electron hole recombination.

Experimental

Chemicals

Bismuth (III) oxide (99.9999% Acros Organics), vanadium(IV) oxide (99+% Strem Chemicals), cobalt(II, III) oxide (Puratronic 99.9985%, Alfa Aesar), cobalt(II) nitrate hexahydrate (98+%, Aldrich) and silver nitrate (99.9+%, Alfa Aesar) were used as received. Acetic acid (glacial, Macron) and nitric acid (68%-70%, EMD) were used after proper dilution. Sodium metaperiodate (98%, Alfa Aesar) was used after recrystallization. Water was purified to $18 \text{ M}\Omega\cdot\text{cm}$ resistivity by a Nanopure II system.

Synthesis

BiVO_4 was synthesized via a revised solid-solution method⁵ at room temperature. 1.15 g (2.5 mmol) of Bi_2O_3 and 0.42 g (5 mmol) of VO_2 were vigorously stirred in 25 mL 1 M aqueous acetic acid solution, at room temperature for 11 days. The obtained powder was washed with 50 mL of water for 3 times, then 50 mL of 0.5 M nitric acid and then again with 50 mL of water for 3 times. The washed powder was vacuum dried and calcined at 673 K for 5 hours in air.

Co_3O_4 was loaded by three different methods. In the first method, 200 mg BiVO_4 powder was soaked in 10 mL aqueous solution of 9.9 mg $\text{Co}(\text{NO}_3)_2 \cdot 6\text{H}_2\text{O}$ (equivalent to 2 mg of cobalt), and dried at about 353 K with slow stirring. The

mixture was then calcined at 673 K for 5 hours. The obtained powder (Chem- Co_3O_4 - BiVO_4) was washed with water and vacuum dried. In the second method, 200 mg BiVO_4 powder was ground together with 2.7 mg Co_3O_4 (equivalent to 2 mg of cobalt) for 10 minutes. The powder mixture was calcined at 673 K in air for 5 hours, washed with 50 mL of water and vacuum dried, to give Phys- Co_3O_4 - BiVO_4 as a brown-yellow powder. Lastly, Echem- Co_3O_4 - BiVO_4 was prepared as described in the main text.

Characterization

Transmission electron microscopy (TEM) images were taken with a Philips CM-12 TEM with accelerating voltage of 120 kV . To prepare the samples, copper grids with carbon film were dipped into aqueous dispersions of the catalysts, washed with pure water and dried in air.

Powder X-ray diffraction patterns were recorded with a Scintag XRD at the wavelength of 0.154 nm , with 2 mm tube slit divergence, 4 mm scatter, 0.5 mm column scatter and 0.2 mm receiving widths. The sizes of the nanoparticles were calculated with the Scherrer equation using the five most intense peaks in each diffraction spectrum, and values were then averaged.

UV-Vis diffuse reflectance spectra were recorded on thin films using a Thermo Scientific Evolution 220 Spectrometer, equipped with an integrating sphere. To prepare the samples, the aqueous dispersions of the catalysts were drop-coated on white Teflon tape and then dried in air. The reflectance data were converted to the Kubelka-Munk function $f(R) = (1-R)^2(2R)^{-1}$ to approximate absorbance.

Surface photovoltage Spectroscopy (SPS) measurements were conducted using a vibrating gold Kelvin probe (Delta PHI Besocke) mounted inside a home-built vacuum chamber ($<1 \times 10^{-4} \text{ mbar}$). To prepare the samples, aqueous dispersions of 0.5 mg catalysts were drop-coated onto F/SnO_2 substrates (MTI Corporation, resistivity = $12\text{-}14 \text{ ohm sq}^{-1}$), dried in air to form thin films and annealed at 673 K for 5h. Samples were illuminated with monochromatic light from a 175 W Xe lamp filtered through an Oriel Cornerstone 130 monochromator and the light intensity range is 0.1 to 0.3 mW/cm^2 . The CPD spectra were corrected for drift effects by subtracting dark scan background recorded prior to the light measurement. No correction for the variable light intensity from the Xe lamp was performed.

Photocatalytic oxygen evolution tests were performed by dispersing 50 mg of the catalysts in 50 mL 0.02 M sodium metaperiodate aqueous solution or 50 mL 0.05 M silver nitrate aqueous solution in a quartz glass flask. The flask was purged with argon several times and the solution mixture was irradiated with a 300 W xenon arc lamp using a 400 nm long pass filter (380 mW cm^{-2} at the flask surface as measured by an International Light IL1400BL photometer equipped with a GaAsP detector). The air-tight irradiation system was connected to a Varian 3800 gas chromatograph (with a $60/80 \text{ \AA}$ molecular sieve column and thermal conductivity detector) to measure the amount of evolved gases.

Photoelectrochemical measurements were conducted in a 3-electrode cell with a Pt counter electrode and a saturated calomel reference electrode connected to the cell with a KCl salt bridge. The cell was filled with 50 mL 0.1 M K₂SO₄. The solution was purged with N₂ to remove oxygen. The scans were recorded under 435 nm LED illumination (intensity 7.4 mW cm⁻²) using a Gamry Reference 600 Potentiostat. For cyclic voltammetry scans, scans were performed in anodic direction with a rate of 10 mV s⁻¹. The cell was calibrated using the standard potential of K₃[Fe(CN)₆] (+0.358 V vs NHE). To prepare the working electrodes, 0.5 mg of the catalysts were drop-coated from aqueous dispersions on 1.0 cm² F/SnO₂ substrates (MTI Corporation, resistivity = 12-14 ohm sq⁻¹), dried in air at room temperature and annealed at 673 K for 5 hours.

Acknowledgements

We are grateful for financial support from Research Corporation for Science Advancement (Scialog Award) and from the National Science Foundation (NSF, Grants 1152250 and 1133099).

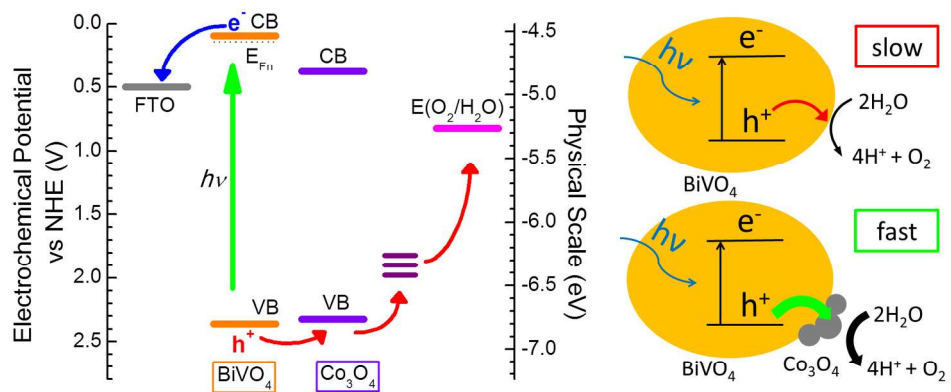
Notes and references

^a Department of Chemistry, University of California, Davis, USA †
Electronic Supplementary Information (ESI) available: [X-ray diffraction patterns, SEM images, Butler-Ginley calculation of flat-band potentials, comparison of oxygen evolution catalysts and calculation of sun light intensity]. See DOI: 10.1039/b000000x/

- F. E. Osterloh, *Chem. Mater.*, 2008, **20**, 35-54.
- D. Yamasita, T. Takata, M. Hara, J. N. Kondo and K. Domen, *Solid State Ionics*, 2004, **172**, 591-595.
- A. Kudo and Y. Miseki, *Chem. Soc. Rev.*, 2009, **38**, 253-278.
- B. A. Pinaud, J. D. Benck, L. C. Seitz, A. J. Forman, Z. Chen, T. G. Deutsch, B. D. James, K. N. Baum, G. N. Baum, S. Ardo, H. Wang, E. Miller and T. F. Jaramillo, *Energy & Environmental Science*, 2013, **6**, 1983.
- F. F. Abdi, L. H. Han, A. H. M. Smets, M. Zeman, B. Dam and R. van de Krol, *Nat. Commun.*, 2013, **4**.
- A. Kudo, K. Ueda, H. Kato and I. Mikami, *Catal. Lett.*, 1998, **53**, 229-230.
- A. Kudo, K. Omori and H. Kato, *J. Am. Chem. Soc.*, 1999, **121**, 11459-11467.
- S. Tokunaga, H. Kato and A. Kudo, *Chem. Mater.*, 2001, **13**, 4624-4628.
- G. C. Xi and J. H. Ye, *Chem. Commun.*, 2010, **46**, 1893-1895.
- M. C. Long, W. M. Cai and H. Kisch, *Journal of Physical Chemistry C*, 2008, **112**, 548-554.
- D. N. Ke, T. Y. Peng, L. Ma, P. Cai and K. Dai, *Inorg. Chem.*, 2009, **48**, 4685-4691.
- Y. Park, K. J. McDonald and K. S. Choi, *Chemical Society Reviews*, 2013, **42**, 2321-2337.
- F. E. Osterloh, *Chem. Soc. Rev.*, 2013, **42**, 2294-2320.
- S. K. Pilli, T. E. Furtak, L. D. Brown, T. G. Deutsch, J. A. Turner and A. M. Herring, *Energy & Environmental Science*, 2011, **4**, 5028-5034.
- S. K. Pilli, T. G. Deutsch, T. E. Furtak, J. A. Turner, L. D. Brown and A. M. Herring, *Phys. Chem. Chem. Phys.*, 2012, **14**, 7032-7039.
- F. F. Abdi, N. Firet and R. van de Krol, *Chemcatchem*, 2013, **5**, 490-496.
- F. F. Abdi and R. van de Krol, *J. Phys. Chem. C*, 2012, **116**, 9398-9404.
- D. Wang, R. Li, J. Zhu, J. Shi, J. Han, X. Zong and C. Li, *The Journal of Physical Chemistry C*, 2012, **116**, 5082-5089.
- J. A. Seabold and K. S. Choi, *J. Am. Chem. Soc.*, 2012, **134**, 2186-2192.
- S. P. Berglund, D. W. Flaherty, N. T. Hahn, A. J. Bard and C. B. Mullins, *J. Phys. Chem. C*, 2011, **115**, 3794-3802.
- M. Long, W. M. Cai, J. Cai, B. X. Zhou, X. Y. Chai and Y. H. Wu, *J. Phys. Chem. B*, 2006, **110**, 20211-20216.
- S. Trasatti, *Journal of Electroanalytical Chemistry and Interfacial Electrochemistry*, 1980, **111**, 125-131.
- A. Iwase and A. Kudo, *Journal of Materials Chemistry*, 2010, **20**, 7536.
- P. Vanýsek, in *CRC Handbook of Chemistry and Physics*, CRC Press/Taylor and Francis, Boca Raton, FL, 2008.
- A. R. Parent, R. H. Crabtree and G. W. Brudvig, *Chemical Society Reviews*, 2013, **42**, 2247-2252.
- L. Kronik and Y. Shapira, *Surf. Sci. Rep.*, 1999, **37**, 1-206.
- L. Kronik and Y. Shapira, *Surf. Interface Anal.*, 2001, **31**, 954-965.
- M. K. Nowotny, P. Bogdanoff, T. Dittrich, S. Fiechter, A. Fujishima and H. Tributsch, *Mater. Lett.*, 2010, **64**, 928-930.
- T. K. Townsend, N. D. Browning and F. E. Osterloh, *Energy & Environmental Science*, 2012, **5**, 9543-9550.
- J. Zhao and F. E. Osterloh, *J. Phys. Chem. Lett.*, 2014, **5**, 782-786.
- P. Zabel, T. Dittrich, M. Funes, E. N. Durantini and L. Otero, *J. Phys. Chem. C*, 2009, **113**, 21090-21096.
- F. E. Osterloh, M. A. Holmes, L. Chang, A. J. Moule and J. Zhao, *J. Phys. Chem. C*, 2013, **117**, 26905-26913.
- M. Waller, T. K. Townsend, J. Zhao, E. M. Sabio, R. L. Chamousis, N. D. Browning and F. E. Osterloh, *Chem. Mater.*, 2012, **24**, 698-704.
- R. Beranek, B. Neumann, S. Sakthivel, M. Janczarek, T. Dittrich, H. Tributsch and H. Kisch, *Chem. Phys.*, 2007, **339**, 11-19.
- D. Gross, I. Mora-Sero, T. Dittrich, A. Belaidi, C. Mauser, A. J. Houtepen, E. Da Como, A. L. Rogach and J. Feldmann, *J. Am. Chem. Soc.*, 2010, **132**, 5981-+.
- F. A. Frame, T. K. Townsend, R. L. Chamousis, E. M. Sabio, T. Dittrich, N. D. Browning and F. E. Osterloh, *J. Am. Chem. Soc.*, 2011, **133**, 7264-7267.
- C. S. Cheng, M. Serizawa, H. Sakata and T. Hirayama, *Materials Chemistry and Physics*, 1998, **53**, 225-230.
- H. R. Sprunken, R. Schumacher and R. N. Schindler, *Faraday Discuss.*, 1980, **70**, 55-66.
- M. A. Butler and D. S. Ginley, *Journal of The Electrochemical Society*, 1978, **125**, 228.
- A. Gulino and I. Fragalà, *Inorganica Chimica Acta*, 2005, **358**, 4466-4472.
- R. G. Li, H. X. Han, F. X. Zhang, D. G. Wang and C. Li, *Energy & Environ. Sci.*, 2014, **7**, 1369-1376.

Textual abstract for the contents pages:

The high activity of $\text{BiVO}_4/\text{Co}_3\text{O}_4$ was attributed to the electrocatalytic properties of the Co_3O_4 cocatalyst and to the formation of heterojunction at the BiVO_4 - Co_3O_4 interface.



447x222mm (120 x 120 DPI)